Research on the Effect of Psammotherapy on the Pulsating Flow of Conical Curved Femoral Artery

Rongchang Fu[a] and Xiaoke Han[b]
School of Mechanical Engineering, Xinjiang University, Huarui Street777, Urumqi, China

Abstract: **Objective** This paper is to study the effect of psammotherapy on the hemodynamicsof the conical curved tube of the femoral artery in humans, and further reveal the mechanism of psammotherapy from the perspective of hemodynamics. **Methods** Based on CT images of the human aorta, a three-dimensional finite element model of the conical curved tube of the femoral artery was established, and the heart rate, the peak velocity and the inner diameter of the femoral artery measured in the experiment were used as initial conditions and boundary conditions for finite element numerical simulation, then the blood flow velocity, wall shear stress and Von Mises stress of curved blood vessels before and after psammotherapy were obtained and compared. **Results** The blood flow velocities of the conical curved femoral artery increased by 18%, 29%, 19% and 45% at t=0.15 min, 0.30 min, 0.45 min and 0.60 min after psammotherapy compared with before psammotherapy; the flow velocity of secondary reflux was significantly weakened, and the wall shear stress increased by 18%, 5%, 13%, and 14%, respectively; Von-Mises stress increased by 189%, 115%, 84%, and 338%, respectively. **Conclusion** Research shows that psammotherapy can improve the fluidity of the femoral artery blood and increase the wall shear stress, which has a corresponding improvement effect on the prevention of the deposition of substances in the arteries; the phenomenon of secondary reflux velocity after psammotherapy is significantly reduced to avoid the deposition of substances in the blood, and it has a certain clinically positive effect on preventing the formation of atherosclerosis, but after psammotherapy , the Von-Mises equivalent stress increases and the increase is also relatively large, indicating that psammotherapy has a potential risk of vascular rupture.

1 INTRODUCTION

With the acceleration of the pace of modern life, people's pressure is increasing rapidly, and the body and mind are exhausted. Therefore, physical therapy has attracted more and more attention. Psammotherapy derived from the unique warm temperate arid desert climate in Turpan, Xinjiang, China is a kind of physical therapy. As it has no side effects, and can improve blood circulation, promote metabolism, and strengthen the body, loses weight, beauty, and health care, it is loved by lots of people. According to statistics, there are about 50,000 people who have psammotherapy in the psammotherapy center of Turpan Uyghur Hospital every year. Psammotherapy is a method of curing diseases by

burying sand. Its principle is to use the naturally formed magnetic sand to comprehensively act on the human body through heat transfer, magnetic field action, and sand action force, so as to get rid of illness and keep fit (Kurban 2011). The influencing factors of psammotherapy are complex and involve many disciplines, so it is difficult to explore the mechanism of its curative effect. Scholars at home and abroad have carried out research on the curative effect mechanism of psammotherapy from the aspects of heat transfer, bone mechanics, clinical medicine, etc. Nyazi Aishan (Niaz 2002) research has shown that psammotherapy is effective for various types of Osteoarthrltis (OA) and other types of rheumatic diseases. In addition, changes in hemorheology indicators are correlated with the occurrence,

[a] https://orcid.org/0000-0002-7045-7597

[b] https://orcid.org/0000-0001-6587-0574

development, treatment and prevention of OA (Chang, Chang, Xu 2009), therefore, relevant scholars are engaged in research to reveal the therapeutic mechanism of psammotherapy from hemorheology and hemodynamics. Wei Rong et al. (Wei, Mahemuti, Yang 2009) studied the hemorheology and hemodynamics of rabbit knee osteoarthritis through experiments in New Zealand rabbit, their research has pointed out that psammotherapy can improve the whole blood viscosity index of model animals; in addition, it can speed up the blood flow in the femoral artery of the lower limbs at the sand-buried site and reduce vascular resistance. Bureby Yiming et al. (Yiming, Fu 2016) studied the effect of psammotherapy on the hemodynamics of the human femoral artery bifurcation under the condition of fluid-solid coupling. However, in the current study to reveal the mechanism of psammotherapy curative effect from the perspective of hemodynamics, the three-dimensional finite element model of blood vessels has not been taken into account the taper of blood vessels, and the blood was supposed as Newtonian fluid. Moreover, arterial diseases mostly occur at the places where the geometric shape of arteries changes, namely, the stenosis, bifurcation and curvature of vessels (Xu, Guo, Wang 2017). Therefore, exploring the influence of psammotherapy on the hemodynamics of conical curved tubes based on non-Newtonian fluids is one of the focuses of this paper. Based on the experimental research, this paper studies the distribution of blood flow field, wall shear stress and Von-Mises equivalent stress in the conical vessel of the femoral artery before and after psammotherapy based on non-Newtonian fluids, so as to provide a theoretical basis for revealing the therapeutic mechanism of psammotherapy on vascular diseases.

2 MATERIALS AND METHODS

2.1 Geometric Model

CT was used to collect real human lower limb images, apply medical image processing software to extract femoral artery blood vessels, and then reverse engineering method (Schulze-Bauer, Morth, Holzapfel 2003) was applied to segment and smooth the femoral artery conical tube, and the three-dimensional reconstruction model of the fluid domain (blood flow) of the blood vessel was constructed under the condition of maintaining the original physiological and anatomical characteristics. The reverse engineering method reference (Zhang, Zhang, Gao 2002) was used to study the femoral artery. a blood vessel wall with a thickness of 1 mm was constructed, and a three-dimensional geometric model of the blood vessel wall was obtained, as shown in Figure 1. The place where the geometric shape of the conical curved femoral artery changes is prone to more complicated flow conditions (Yang, Yu, Liu, Hong 2014), and many vascular and blood diseases often occur in such places, so the inner and outer sides of the conical curved femoral artery were selected as monitoring points. The inner monitoring points are A, B, C, D and the outer monitoring points are a, b, c, d, and they are distributed along the taper, mainly to monitor the time-varying fluid velocity of these points.
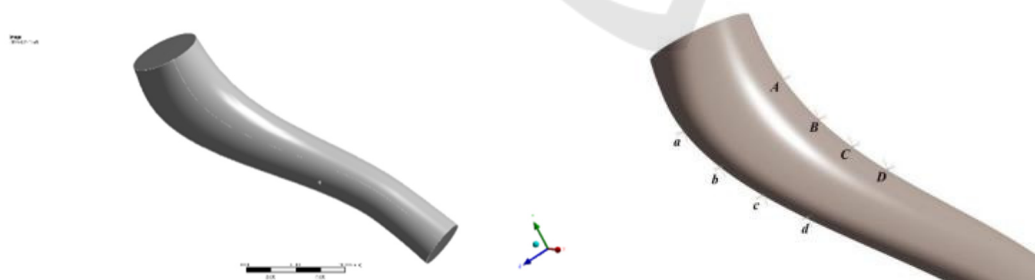
Figure 1: Three-dimensional geometric model of blood vessel.

2.2 Finite Element Calculation

The finite element analysis software ICEM meshing was used for meshing, and ANSYS 18.0 was used for bidirectional fluid-solid coupling analysis. The fluid-solid coupling calculation mainly used the fluid solver and the solid structure solver to calculate the fluid-solid interaction problem at the same time. The fluid solver mainly calculated physical quantities such as pressure, velocity, temperature, and composition of the flow field, while the solid structure solver calculated physical quantities such as displacement, stress, and strain. Among these solution variables, the physical quantities that exist in

both fluid and solid solutions were pressure and displacement. In the fluid solver, the pressure was the direct solution, while in the solid solver, the pressure can be used as a load. In the solid solver, the displacement was the direct solution quantity, while in the fluid solver, the displacement can be used as a load, which is expressed as a calculation domain motion or deformation.

2.3 Initial Conditions, Boundary Conditions and Material Properties

The blood flow is a pulsating flow, which was achieved by setting the initial speed of the pulsation in this paper. According to the experimental results of the research group, the subjects were selected from a healthy group of 22~27 years old, a total of 59 people. Among them, 26 males were 172~176 cm tall and weighed 67~75 kg; 33 females were tall and weighed 46~60 kg. After signing the informed consent form with the subject, the psammotherapy test was carried out. Each psammotherapy time was 30 minutes, once a day, and 15 days was a course of treatment. SPSS software was used to process the peak blood flow velocity, inner diameter and heart rate before and after femoral artery psammotherapy (as shown in Table 1). As $T = \dfrac{60}{heart\ rate}$, $\omega = \dfrac{2\pi}{T}$,the angular velocity was determined. Since the pulsation velocity can be considered to change according to a sine function within a pulsation cycle, the initial condition of the femoral artery was set as the pulsating blood flow velocity (Yiming, Fu 2017), that is, $v_{in} = 0.93\ sin(7.99t)$, $v_{out} = 1.23\ sin(9.70t)$; the outlet pressure was set to p = 0 . The boundary conditions of the femoral artery wall were set to have no penetration and no slip boundary.

The blood vessel wall was set an incompressible isotropic material (Liu，Wu，Dhanjoo 2015), and its density $\rho_{soild} = 1150\ kg/m^3$, Elastic modulus, $E = 5Mpa$ and Poisson's ratio $\nu = 0.45$ The density of blood $\rho_{blood} = 1.05 \times 10^3\ kg/m^3$.

Table 1: Femoral artery hemodynamic indexes before and after psammotherapy (n = 59).

parameter	Before psammotherapy	After psammotherapy
speed /(cm·s-1)	92. 51 ± 8. 87	122. 51 ± 16. 98
Inner diameter /cm	0. 76 ± 0. 11	0. 78 ± 0. 11
Heart rate	76. 32 ± 11. 40	92. 69 ± 16. 09
Cardiac cycle /s	0. 789 0	0. 651 6

2.4 Governing Equation

A large number of studies have shown that animal blood has the characteristics of non-Newtonian fluid, and the shear force and shear strain rate of blood are nonlinear. Here we set the blood as an incompressible non-Newtonian fluid, select the non-Newtonian flow model, and the flow control equation (Matos，Oliveira 2013) is:

$$\nabla \cdot u = 0 \qquad (1)$$

$$\rho \frac{\partial u}{\partial t} + \rho(u\square\nabla)u = -\nabla p + \nabla\square\bar{\tau} \qquad (2)$$

In the formula, the stress tensor $\bar{\tau}$ and the strain rate tensor $\bar{\gamma}$ are nonlinear relations:

$$\bar{\tau} = \mu(|\bar{\gamma}|)\bar{\gamma} \qquad (3)$$

This paper selects the model of Carreau-Yasuda (Morales, Larrabide, Geers, Aguilar, Frangi 2013):

$$\mu = \mu_\infty + (\mu_0 - \mu_\infty)\left[1 + (\lambda\gamma)^z\right]^{(n-1)/z} \qquad (4)$$

According to the literature, parameters are respectively set as $\lambda = 0.110s$, $n = 0.392$, $\mu_0 = 22\times10^{-3}\ pa\cdot s$, $\mu_\infty = 2.2\times10^{-3}\ pa\cdot s$, $z = 0.644$, dynamic viscosity μ

In addition, the control equation of the blood vessel wall model (Chatziprodromou, Tricoli, Poulikakos, Ventikos 2007) is expressed as follows:

$$\nabla \cdot \sigma_{ij} = \rho_s a_s \qquad (5)$$

Here σ_{ij} represents the stress tensor of the blood vessel wall; a_s represents the acceleration of the blood vessel wall; ρ_s represents the density of the blood vessel wall.

When the coupling between the fluid and the solid occurs, the contact surface between the fluid and the solid needs to establish a corresponding relationship to meet this condition. Fluid and solid will transmit displacement and speed through the contact surface

between them. The following conditions should be met on the contact surface between fluid and solid:

$$\begin{cases} d_s = d \\ \sigma_{ij} \cdot n_s = T \cdot n \\ U_s = U \end{cases} \quad (6)$$

In these equations, the subscript s represents the physical quantity of the blood vessel wall; n represents the boundary normal; d represents the displacement.

3 RESULT

3.1 Distribution of Blood Flow Field before and after Psammotherapy

(1).t=0.15s (2).t=0.30s (3).t=0.45s (4).t=0.60s

A. Before psammotherapy

(1).t=0.15s (2).t=0.30s (3).t=0.45s (4).t=0.60s

B. After psammotherapy

Figure 2: Velocity distribution cloud diagram in the conical curved femoral artery.

Figure 2 shows the velocity distribution cloud map of the tapered femoral artery during a cardiac cycle. Figure 2A is the cloud map of different instantaneous velocity distributions before psammotherapy, and Figure 2B is the cloud map of different instantaneous velocity distributions after psammotherapy. Figure 2 shows that, before psammotherapy, the central area of the front blood flow velocity moves to the inside to a certain extent, resulting in a low velocity area on the outside of the blood vessel, so vortexes are generated in this area. Compared with before psammotherapy, the gradient of blood flow velocity in the radial direction of the conical femoral artery curve is less drastic after sand therapy, and the possibility of bidirectional eddy is reduced; the blood flow field is more evenly distributed after psammotherapy than before psammotherapy, and the resulting low-velocity area is decreasin.

Table 2 is a comparison table of the maximum speed before and after psammotherapy. The relative change of the maximum speed is the absolute change of the same instantaneous maximum speed before and after psammotherapy divided by the percentage of the maximum speed before psammotherapy. Table 2 shows that the maximum speed after psammotherapy is higher than that before psammotherapy. The maximum speeds of before and after psammotherapy are reached at 0.30s, and the absolute change of the maximum speed is also the largest. The relative change of the maximum speed is the largest at 0.60s.

Figure 3 shows the speed change with time curve of the conical curved femoral artery of the inner monitoring point A~D and the outer monitoring point a~d. It is found that the speed of the inner side of the bend changes significantly with time before psammotherapy, while the inner speed change after

psammotherapy is relatively gentle, the difference between these points is not obvious, and the average maximum value is also reduced; the blood flow velocity at some points before the curved lateral psammotherapy is lower, and the blood flow speed increases after the psammotherapy, but the variation range of blood flow velocity after sand therapy is relatively small compared with that before psammotherapy, and the flow is relatively smooth.

Table 2: Comparison of maximum speed before and after psammotherapy.

Time (s)	Maximum speed before psammotherapy (m/s)	Maximum speed after psammotherapy (m/s)	Absolute change of maximum speed (m/s)	Relative change of maximum speed (%)
0.15	2.48	2.92	0.44	18
0.30	3.23	4.16	0.93	29
0.45	2.26	2.69	0.43	19
0.60	0.44	0.64	0.2	45
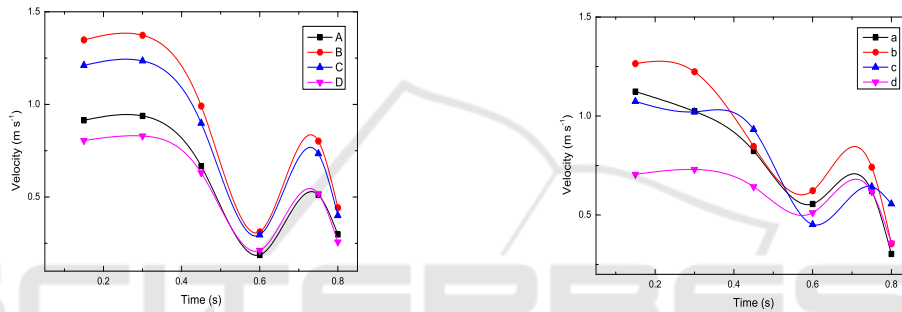
A. Before psammotherapy
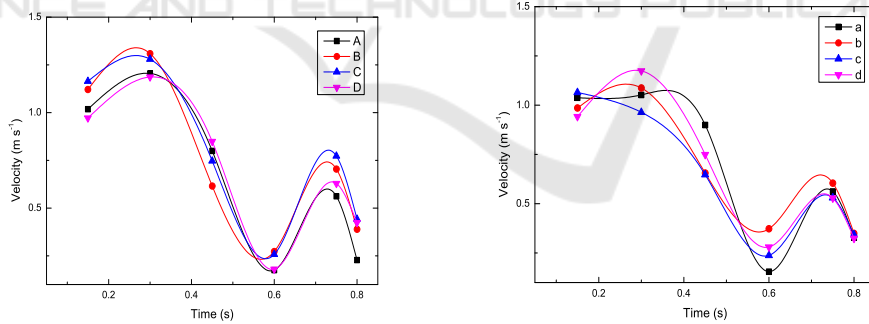
B. After psammotherapy

Figure 3.

3.2 Wall Shear Stress Distribution before and after Psammotherapy

Figure 4A is the distribution diagram of wall shear stress with time before psammotherapy, and Figure 4B is the distribution cloud diagram of wall shear stress with time after psammotherapy. Figure 4 shows that, at the curve of conical vessels, the blood first decompresses and speed increases, then its speed decelerates and pressurizes, and finally the boundary layer falls off, so that the velocity changes greatly, and the shear stress of the blood vessel wall is also more obvious. As the taper of the blood vessel increases, the wall shear stress caused by the acceleration of the flow speed also gradually increases. Compared with before psammotherapy , the blood vessel wall shear stress distribution after psammotherapy is more uniform overall.

Table 3 is a comparison table of the maximum wall shear stress before and after psammotherapy. The relative change of the maximum wall shear stress is the absolute change of the maximum wall shear stress at the same instant before and after psammotherapy divided by the percentage of the maximum wall shear stress before psammotherapy.

Table 3 shows the maximum wall shear stress after psammotherapy is higher than the maximum wall shear stress before psammotherapy. When 0.30s, the maximum wall shear stress before and after psammotherapy is the largest, but the maximum absolute change of the maximum wall shear stress occurs at 0.15s, and the relative change of the maximum wall shear stress is the largest at 0.15s.

(1).t=0.15s (2).t=0.30s (3).t=0.45s (4).t=0.60s

A. Before psammotherapy

(1).t=0.15s (2).t=0.30s (3).t=0.45s (4).t=0.60s

B. After psammotherapy
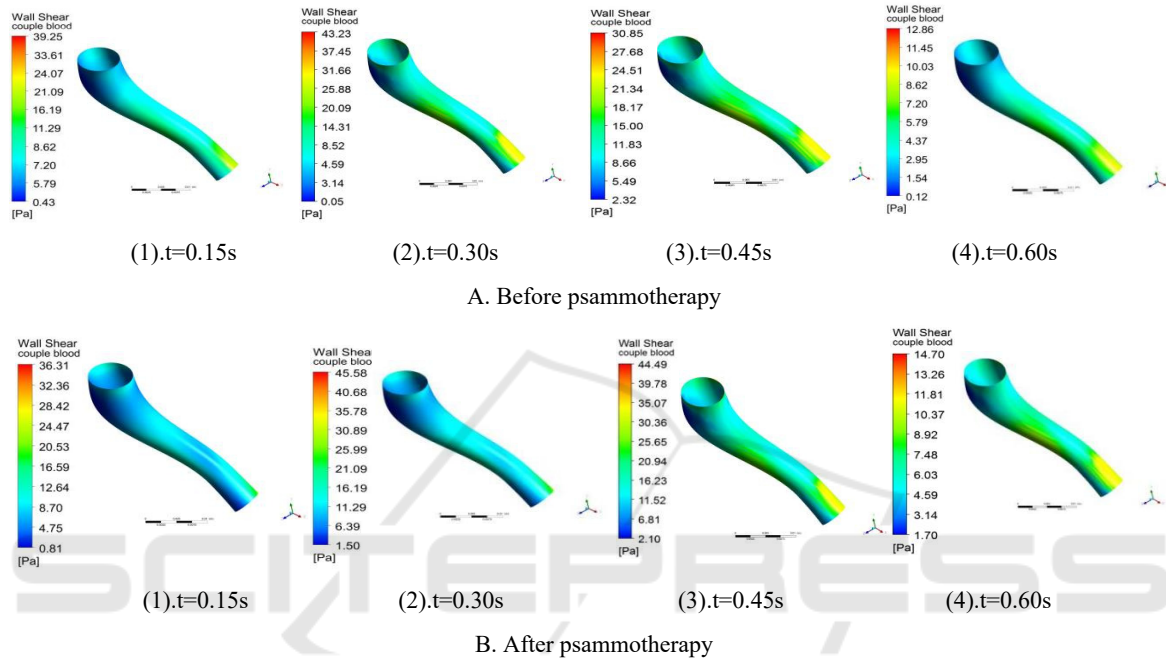
Figure 4: Cone-curved artery wall shear stress distribution cloud map.

Table 3: Comparison of maximum wall shear stress before and after psammotherapy.

Time (s)	Maximum wall shear stress before psammotherapy (Pa)	Maximum wall shear stress after psammotherapy (Pa)	Absolute change of maximum wall shear stress (Pa)	Relative change of maximum wall shear stress (%)
0.15	30.85	36.31	5.46	18
0.30	43.23	45.58	2.35	5
0.45	39.25	44.49	5.24	13
0.60	12.86	14.70	1.84	14

3.3 Vascular Von-Mises Equivalent Stress Distribution before and after Psammotherapy

The blood vessel is an elastic body. Under the coupling action of the blood vessel and the blood, the blood vessel will produce a certain deformation. The Von-Mises equivalent stress distribution of blood vessels before and after psammotherapy is shown in Figure 5. The Von-Mises equivalent stress is the stress for judging whether the material has yielded, and its expression is $\sigma_{r4} = \sqrt{\frac{1}{2}[(\sigma_1 - \sigma_2)^2 + (\sigma_2 - \sigma_3)^2 + (\sigma_3 - \sigma_1)^2]}$, where σ_1, σ_2, σ_3 are the three principal stresses of the dangerous point.

When the Von-Mises stress is less than the yield stress, the material is in elastic state, otherwise it is plastic state. Figure 5 shows that the Von-Mises stress on both sides of the vessel with the largest curvature

(1).t=0.15s   (2).t=0.30s   (3).t=0.45s   (4).t=0.60s

A. Before psammotherapy

(1).t=0.15s   (2).t=0.30s   (3).t=0.45s   (4).t=0.60s

B. After psammotherapy
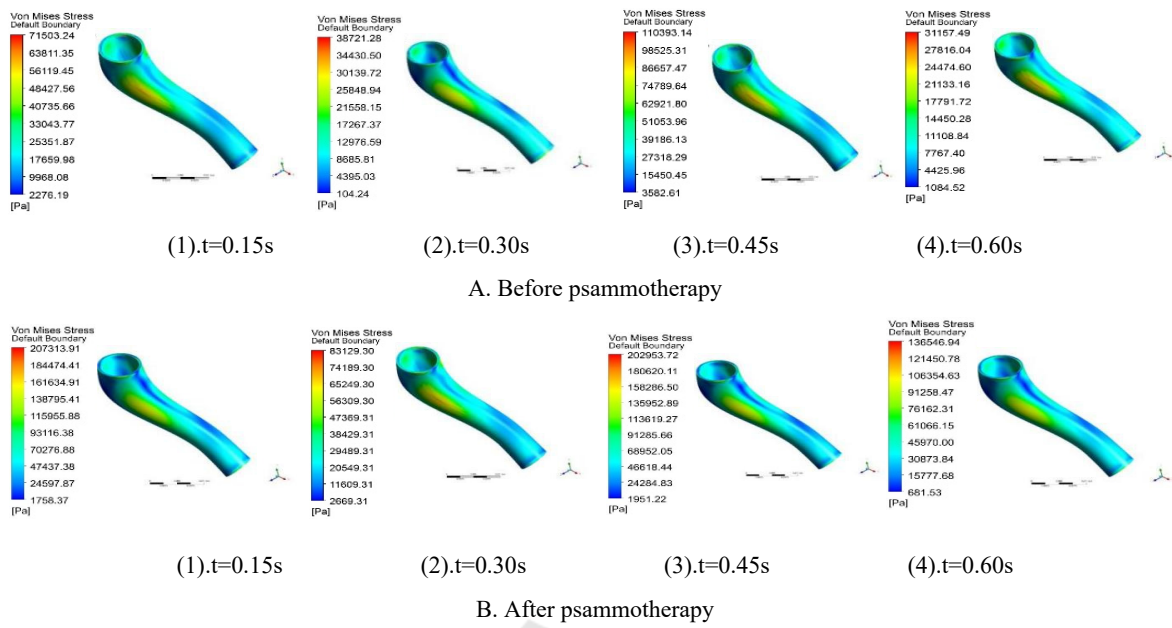
Figure 5: Von-Mises equivalent stress distribution cloud diagram of conical curved artery.

Table 4: Comparison of maximum Von-Mises equivalent stress before and after psammotherapy.

Time (s)	Maximum Von-Mises equivalent stress before psammotherapy (kPa)	Maximum Von-Mises equivalent stress after psammotherapy (kPa)	Maximum absolute change of Von-Mises equivalent stress (kPa)	Maximum relative change of Von-Mises equivalent stress (%)
0.15	71.50	207.31	135.81	189
0.30	38.72	83.13	44.41	115
0.45	110.39	202.95	92.56	84
0.60	31.16	136.55	105.39	338

is the largest, and the distribution law before and after psammotherapy is basically the same.

Table 4 is the comparison table of the maximum Von-Mises equivalent stress before and after psammotherapy. The maximum relative change of Von-Mises equivalent stress is the absolute change of the same instantaneous maximum Von-Mises equivalent stress before and after psammotherapy divided by the percentage of Von-Mises equivalent stress of the maximum before psammotherapy.

Table 4 shows that the maximum Von-Mises equivalent stress after psammotherapy is higher than the maximum Von-Mises equivalent stress before psammotherapy. The maximum Von-Mises equivalent stress is at 0.45s before psammotherapy. The effect force reaches the peak value of 110.39kPa, the maximum Von-Mises equivalent stress reaches the peak value of 207.31kPa at 0.15s after psammotherapy, and the maximum absolute change of the maximum Von-Mises equivalent stress occurs at 0.15s, and its value is 135.81kPa. The maximum relative change of the maximum Von-Mises equivalent stress occurs at 0.6s, and its value is 338%.

4 CONCLUSIONS

After psammotherapy, the blood flow field changes, the blood flow velocity increases, and the blood flow field is improved. Compared with before psammotherapy, the speed gradient of blood flow is relatively weakened at the conical bend, and the blood flow field distribution is relatively even compared with before psammotherapy. After psammotherapy, the blood flow velocity changes relatively smoothly

and the blood flow velocity increases in the conical curve, which can effectively prevent the deposition of large substances in the blood, so that the large substances can be transported with the blood, and the shear stress of blood vessel wall increases effectively to prevent the thickening of blood vessel wall after psammotherapy. Studies on blood flow velocity and wall shear stress show that psammotherapy has a positive effect on preventing the formation of atherosclerosis. However, after psammotherapy, the von-Mises equivalent stress increased, and this increase is relatively large and has a potential risk of vascular rupture.

This paper considers the non-Newtonian characteristics of blood, and the reverse CT scan of the human blood vessel model can effectively approach the physiological conditions of the human body. However, there are still shortcomings in the calculation. As we all know, blood is not just plasma, but also includes blood cells and other substances, which makes it become a multiphase flow problem. To be more similar to the real human body, these problems will be all considered in future research.

ACKNOWLEDGEMENTS

REFERENCES

Abdul Saramu·Sidura·Usman·Yasheng Shatar·Kurban, (2011) The characteristics and mechanism of sand burial therapy, Chinese Journal of Ethnic Medicine, No. 9, P54-56

Bureby Yiming, Fu Rongchang. (2016) Hemodynamic effects from sand therapy of Uyghur medicine on the branch of femoral artery[J]. Journal of Medical Biomechanics, 31(05): 431-436.

Bureby Yiming, Fu Rongchang. (2017) Numerical simulation of two-way fluid-solid coupling hemodynamics of femoral artery under Uyghur medicine psammotherapy [J]. Chinese Journal of Biomedical Engineering, 36(04): 507-511.

Chang Yongchao, Chang Yanqing, Xu Deying, (2009) Changes of hemorheological indexes in patients with osteoarthritis, Orthopedics of Traditional Chinese Medicine, Volume 21, Issue 9, P35-36

Chatziprodromou I, Tricoli A, Poulikakos D, Ventikos Y. (2007) Haemodynamics and wall remodelling of a growing cerebral aneurysm: a computational model[J]. Journal of Biomechanics 40 (2): 412-426.

Liu Guiying, Wu Jianhuang, Dhanjoo N G, et al. (2015) Hemodynamic characterization of transient blood flow in right coronary arteries with varying curvature and side - branch bifurcation angles [J]. Computers in Biology and Medicine, 64: 117-126.

Matos H M, Oliveira P J. (2013) Steady and unsteady non-Newtonian inelastic flows in a planar T-junction[J]. International Journal of Heat and Fluid Flow, 39: 102-126.

Morales H G, Larrabide I, Geers A J, Aguilar M L, Frangi A F. (2013) Newtonian and non Newtonian blood flow in coiled cerebral aneurysms [J]. Journal of Biomechanics, 46 (13): 2158-2164.

Niaz Aishan, (2002) Research on the treatment of rheumatism with psammotherapy in Turpan, Xinjiang, Chinese Journal of Ethnic Medicine, Issue 1, P21-22

Schulze-Bauer CA, Morth C, Holzapfel GA. (2003) Passive biaxial me-chanical response of aged human iliac arteries[J]. J Biomech En-g, 125(3): 395-406.

Wei Rong, Dilinal Mahemuti, Yang Shaoling, (2009) Uyghur psammotherapy on blood rheology and hemodynamics of rabbit knee osteoarthritis[J]. Science & Technology Review, 27(3): P84-86.

Xu Xiangyu, Guo Pan, Wang Xiaofeng, et al. (2017) Using dynamic grid technology to simulate the development of atherosclerosis[J]. Journal of Medical Biomechanics,4(36):336-341.

Yang Jinyou, Yu Hang, Liu Jing, Hong Yang. (2014) A hierarchical model of abdominal aortic aneurysm based on fluid-structure coupling analysis[J]. Biomedical Engineering and Clinics, 4(18):310-314.

Zhang Mei, Zhang Yun, Gao Yuehua. (2002) Comparative study on the normal value of carotid artery and femoral artery intima-media layer thickness[J]. Chinese Medical Imaging Technology, 18(1): 32-33.